Deformation behaviour of two continuously cooled vanadium microalloyed steels at liquid nitrogen temperature

Dragomir M. Glišić, Abdunnaser H. Fadel, Nenad A. Radović, Djordje V. Drobnjak, Milorad M. Zrilić

University of Belgrade, Faculty of Technology and Metallurgy, Belgrade

Abstract

The aim of this work was to establish the deformation behavior of two vanadium microalloyed medium carbon steels with different contents of carbon and titanium by tensile testing at 77 K. Samples were reheated at 1250 °C for 30 min and continuously cooled in still air. Beside acicular ferrite as the dominant morphology in both microstructures, the steel with lower content of carbon and negligible amount of titanium contains considerable fraction of grain boundary ferrite and pearlite. It was found that Ti-free steel exhibits a higher strain hardening rate and significantly lower elongation at 77 K than the fully acicular ferrite steel. The difference in tensile behavior at 77 K of the two steels has been associated with the influence of the pearlite, together with higher dislocation density of acicular ferrite.

Keywords: Co(II) determination, Sn(II) determination, kinetic spectrophotometric method.

Available online at the Journal website: http://www.ache.org.rs/HI/

SCIENTIFIC PAPER

UDC 669.14.01/.09

Hem. Ind. **67** (6) 981–988 (2013)

doi: 10.2298/HEMIND121214015G

Traditional medium carbon forging steels achieve their strength and toughness in additional separate processes of quenching and tempering after forging [1––4]. In order to reduce production costs and avoid usual problems associated with quenching, especially long products, vanadium microalloyed forging steels had been developed [5]. These steels achieve required level of strength during air cooling directly from hot forging temperature, due to V(C,N) precipitation in ferrite. However, the toughness of the air cooled steels is lower, because coarsening of austenite grains at temperatures used in conventional forgings produces coarse ferrite-pearlite structure. Microalloying with titanium provided austenite grain refinement by Zener pinning effect of highly insoluble TiN particles [6,7]. Fine ferrite-pearlite structures with improved toughness had been achieved. On the other hand, coarse TiN particles, usually larger than 1 μm [1], act as fracture nucleation sites and are detrimental to the toughness of the steel.

Further toughness improvement had been achieved in medium carbon Ti–V microalloyed steels with acicular ferrite structure [1–4]. Acicular ferrite, often considered as intragranulary nucleated bainite [8], consists of fine interlocking plates with random crystalographic orientation. It is assumed that acicular ferrite plate boundaries effectively resist propagation of microcracks nucleated at brittle particles [3,9]. However it remains unclear whether it is grain size or particle size that controls cleavage fracture.

Correspondence: D. Glišić, Department of Metallurgical Engineering, Faculty of Technology and Metallurgy, University of Belgrade, Karnegijeva 4, 11120 Belgrade, Serbia.

E-mail: gile@tmf.bg.ac.rs

Paper received: 14 December, 2012

Paper accepted: 29 January, 2013

In order to examine the cleavage process itself in microalloyed medium carbon steels with acicular ferrite structure, and predict fracture behaviour, it is necessary to have knowledge of deformation behaviour in conditions close to nil ductility. Therefore, in the present work, deformation behavior at liquid nitrogen temperature of two medium carbon vanadium microalloyed steels with different amount of carbon and titanium was analyzed by means of tensile testing at liquid nitrogen temperature.

EXPERIMENTAL PROCEDURE

Two commercial medium carbon V-microalloyed steels with different content of carbon and titanium received as hot-rolled rods were investigated. The chemical composition of the steels is given in Table 1, where numbers in labels “A19” and “B22” indicate the rod diameter in milimeters. In order to eliminate as-received microstructure 200 mm long samples were homogenized at 1250 °C for 4 h and quenched in oil. In order to provide homogeneous solid solution, samples were afterward reaustenized at 1250 °C for 30 min and cooled in still air. In all heat treatments, argon was used as a protective atmosphere.

In order to measure previous austenite grain size, the following procedure was applied. After quenching in water, samples were tempered at 450 °C for 24 h, in order to allow phosphorous segregation on previous austenite grain boundaries, and then slowly cooled in still air to room temperature. Polished samples were etched by a solution of 10 g of picric acid ($C_6H_3N_3O_7$), 50 ml of sodium alkylsulfonate and 1 ml of HCl in 100 ml of distilled water. The solution was heated to 90 °C and

Table 1. Chemical composition of the steels (wt.%)

Steel	C	Si	Mn	P	S	Cr	Ni	Mo	V	Ti	Al	Nb	N
A19	0.256	0.416	1.451	0.0113	0.0112	0.201	0.149	0.023	0.099	0.002	0.038	0.002	0.0229
B22	0.309	0.485	1.531	0.0077	0.0101	0.265	0.200	0.041	0.123	0.011	0.017	0.003	0.0228

the samples were immersed for 25 s. Grain size determination was done *via* standard linear intercept method.

The transverse metallographic specimens were polished and etched in a 2% nital solution. Microstructure was examined using optical microscopy.

Cylindrical specimens of 5 mm diameter and 30 mm gauge length were machined and tensile tested at liquid nitrogen temperature at a cross-head velocity of 0.1 mm/min, giving an initial strain rate of $5.5 \cdot 10^{-5}$ s^{-1}.

RESULTS

Microstructure of steel A19 (0.256 wt.% C, 20 ppm Ti) is characterized by dominant presence of acicular ferrite, with some ferrite and pearlite along previous austenite grain boundaries (Figure 1). Within the generally continuous layer of grain boundary ferrite, both polygonal idiomorphs and thin elongated allotriomorphs are present. A few examples of Widmanstätten saw-teeth ferrite emanating from grain boundary ferrite allotriomorphs can also be seen. Fine interlocking structure of acicular ferrite inside prior austenite grain interiors is in many cases separated from the grain boundary ferrites by pearlite. Some inragranullary nucleated coarse plates could be recognized as Widmanstätten ferrite [4], although it is not always easy to distinguish it from the acicular ferrite at optical microscopy level.

Predominant morphology in the microstructure of the steel B22 (0.309 wt.% C, 110 ppm Ti) is acicular ferrite (Figure 2). As opposed to the steel A19, the structure of the steel B22 is almost free of pearlite and the grain boundary ferrite layer is thinner and discon-

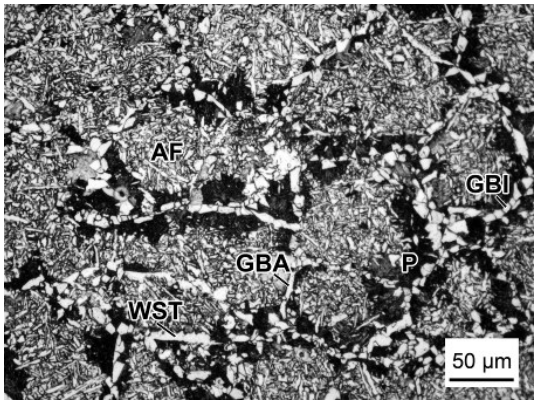

(a)

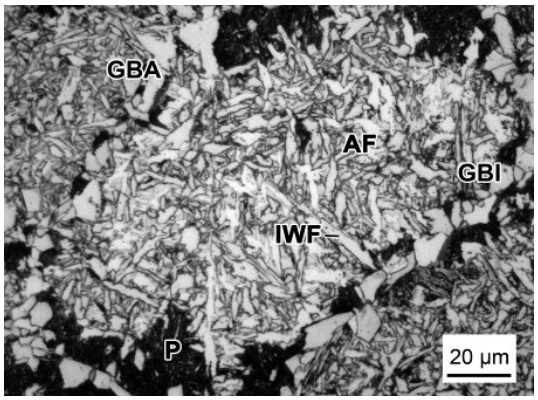

(b)

Figure 1. Microstructure of steel A19 (air-cooled from the austenitization at 1250 °C for 30 min). GBI – grain boundary idiomorph, GBA – grain boundary allotriomorph, P – pearlite, AF – acicular ferrite, WSF – Widmanstätten saw-teeth ferrite, IWF – intragranular Widmanstätten ferrite.

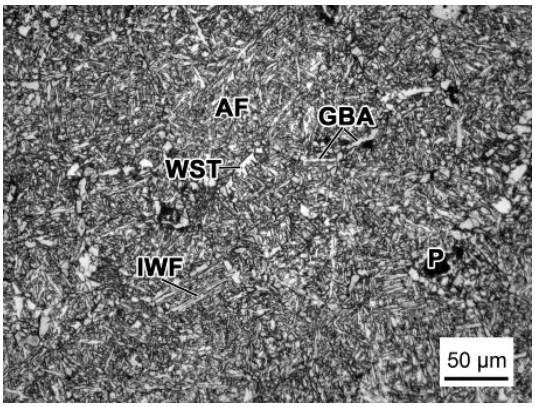

(a)

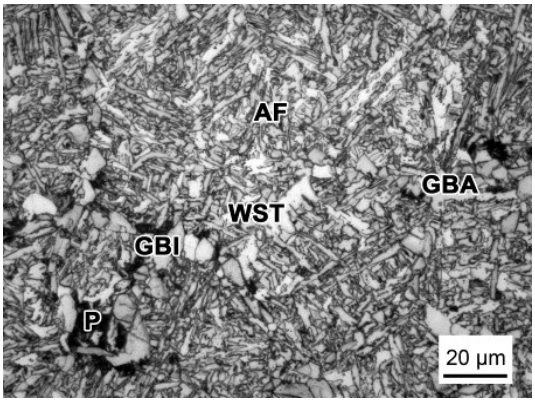

(b)

Figure 2. Microstructure of steel B22 (air-cooled from the austenitization at 1250 °C for 30 min). GBI – grain boundary idiomorph, GBA – grain boundary allotriomorph, P – pearlite, AF – acicular ferrite, WSF – Widmanstätten saw-teeth ferrite, IWF – intragranular Widmanstätten ferrite.

tinuous. Widmanstätten ferrite sideplates nucleated at the grain boundary directly at grain boundary allotriomorphs could be noticed too.

Previous austenite grain size (PAGS) is given in Table 2.

Table 2. Prior austenite grain size in tested steels

Steel	Austenitization, temperature/time	PAGS, μm
A19	1250 °C/30 min	100 ± 10
B22	1250 °C/30 min	80 ± 10

True stress-strain curves for the steels A19 and B22 tested at 77 K are shown in Figure 3. The steel B22 exhibits considerably higher elongation than the steel A19, while the latter show higher level of strain hardening. Instantaneous strain hardening rate as a function of true stress is given in Figure 4 and it demonstrates again higher level of strain hardening for the A19 steel. Stress-strain curves show gradual increase of flow stress, *i.e.*, there is no sharp yield point. Therefore, offset yield strength was established.

Table 3 summarizes tensile properties at 77 K, alongside with the values of yield stress to ultimate tensile stress ratio. Steel B22 exhibit yield stress higher by 123 MPa and ultimate tensile stress by 64 MPa than for steel A19. Total elongation for steel B22 is also higher (10.0 comparing to 5.0%), while steel A19 has a somewhat higher strain hardening index.

DISCUSSION

Microstructure

As shown in Figures 1 and 2, the dominant microstructure in both steels is acicular ferrite, while difference in pearlite content being the dominant difference. Hardenability of steel B22 is higher than for steel

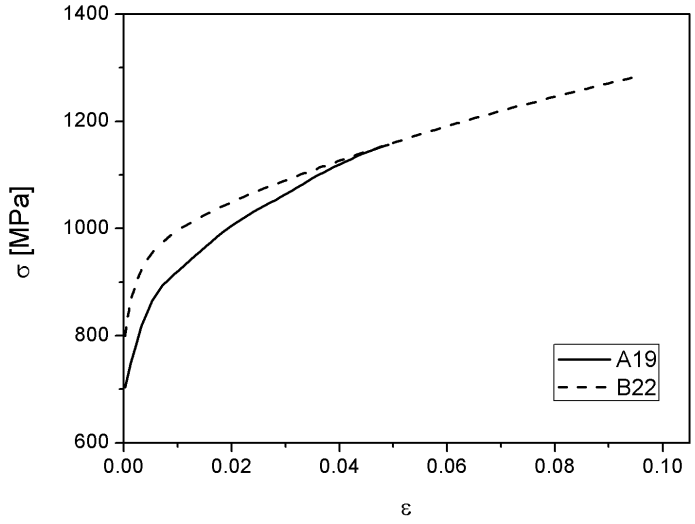

Figure 3. Tensile true stress – true strain curves at 77 K.

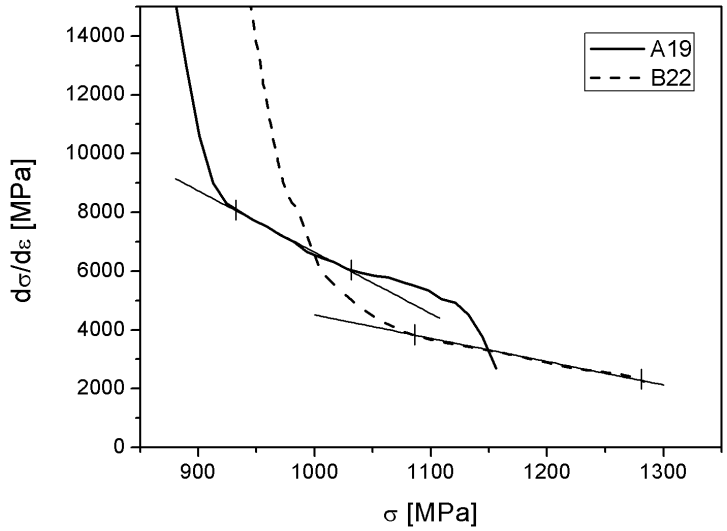

Figure 4. Strain hardening rates as a function of a true stress at 77 K.

Table 3. Tensile properties of the steels tested at 77 K; Room temperature values for the steels with equivalent chemical composition and the same termomechanical treatment is given for comparison

Steel	$\sigma_{0.2}$ / MPa	σ_m / MPa	e_t / %	$\sigma_{0.2}/\sigma_m$	n	Test temperature, K	Ref.
A19	775	1105	5.0	0.70	0.17	77	This work
B22	898	1169	10.0	0.77	0.16	77	This work
Ti-free	531	853	17.0	0.62	-	298	[10]
Ti-V	555	864	18.5	0.64	-	298	[10]

A19, since structure of the latter contains considerable fraction of pearlite. In steel B22 pearlite reaction is for the most part inhibited, even though samples were cooled at still air (about 60 °C/min). Manganese is well known to have the strongest retarding effect on diffusional decomposition of austenite, for elements present in both steels [11-13]. Since its content is practically equal in both steels, the higher hardenability in steel B22 is attributed to higher carbon content. Differences in other alloying element contents are not significant either, except for the titanium. Titanium is added for the purpose of austenite grain refinement and grain size control [6,7]. Its influence on hardenability is indirect, because grain boundaries are preferential nucleation sites for ferrite and pearlite. Bainite also nucleates intergranularly and larger grain sizes will slow down the kinetics in favor of intragranular nucleation. Furthermore, by increasing the grain size the probability of trapping inclusions/precipitates within austenite grain is also enlarged [14,15]. At austenitization temperature of 1250 °C, the measured austenite grain size is 100 μm for steel A19 and 80 μm for steel B22. Such large grain should enhance acicular ferrite formation in detriment of bainite by increasing the ratio between intragranular and grain boundary nucleation sites. However, in the case of the steels studied here, the effect of titanium on hardenability seems to be negligible, considering modest prior austenite grain size difference and that in both steels acicular ferrite intragranular nucleation predominated.

Temperatures for complete dissolution of VN and VC and distribution of main alloying elements are summarized in Table 4. It is assumed that total amount of Ti is contained within TiN particles, which are insoluble at reheating temperature of 1250 °C. Distribution of alloying elements was calculated assuming that on cooling from austenitization temperature precipitation of VN particles precedes VC precipitation and also taking into account stochiometric ratios of Ti:N = 3.4 and V:N = 3.6. Excess vanadium is available for VC precipitation or solid solution strengthening. It is assumed that VC does not precipitate separately from VN, but in fact as V(C,N) [16]. Temperatures for complete dissolution of VN and VC were calculated using equations for solubility products [17]:

$$\log[V][N] = -7840/T_{VN} + 3.02 \quad (1)$$

$$\log[V][C] = -9500/T_{VC} + 6.72 \quad (2)$$

Vanadium-nitride particles are favorable sites for nucleation of acicular ferrite [3,18,19]. Nitrogen available after TiN precipitation during solidification of the steels is available for VN precipitation. The reheating temperature of 1250 °C is above the temperature for complete dissolution of VN and taking into account similar values of vanadium content in both steels, quantity of VN particles should not be significantly different. According to the balance of Ti, V and N content (Table 4), all nitrogen is spent by precipitation of the alloying elements and thus vanadium is in excess. It was reported that vanadium solutes segregation render prior austenite grain boundaries inactive for nucleation of grain boundary ferrite [20], similarly to the well-known effect of boron [21]. Baring in mind precipitation of VC at lower temperatures than for VN, significant amount of free vanadium solute in steel A19 is not expected ($[V]_{excess}$ = 0.018 wt.%), as opposed to the steel B22 where excess amount of vanadium is higher ($[V]_{excess}$ = 0.052 wt.%) and some vanadium in solid solution could be expected. Nevertheless, it seems that vanadium solutes in steel B22 did not affect the nucleation of grain boundary ferrites and therefore its influence on hardenability is not conclusive.

Mechanical properties

Higher yield strength of the steel B22 is an understandable consequence of higher carbon content than in steel A19. The observed gradual yielding, typical for bainitic structures, is mainly due to higher density of mobile dislocations [8]. Multiple phases in structure with marked difference in strength can also contribute gradual yielding, because only the softer phase would

Table 4. Temperatures for complete dissolution of VN and VC and distribution of V, Ti and N

Steel	T_{VN} / °C	T_{VC} / °C	[V] / wt.%	[Ti] / ppm	[N] / ppm	$[N]_{TiN}$ / ppm	$[V]_{VN}$ / wt.%	$[V]_{excess}$ / wt.%	$[N]_{VN}$ / ppm
A19	1108.1	869.2	0.099	20	229	6	0.081	0.018	223
B22	1117.3	893.9	0.123	110	228	32	0.071	0.052	196

deform until it attained the strength of the harder phase [8]. The previously observed effect of yield strength decrease with temperature in bainitic medium carbon steels [22] is actually the effect of continuous-yielding, characteristic for low temperature deformation of these steels (see sketch in Figure 5). It is ascribed to the presence of retained austenite in the structure [22]. Elsewhere authors believe that it is a consequence of the higher mobile dislocation density in bainite, or in this case acicular ferrite [8].

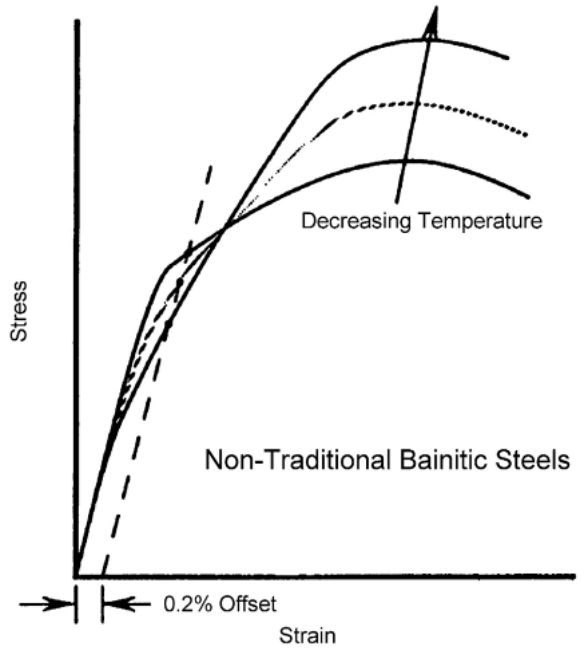

Figure 5. Schematic representatiom of the effect of test temperature on yield point of medium carbon bainitic steels [22].

According to the Kocks-Mecking model the linear part of the $d\sigma/d\varepsilon$-σ curve (stage III hardening) represents the rate of strain hardening decrease [23, 24]. The slope of the linear part of the curve for steel A19 indicates a faster strain hardening decrease than for steel B22. Strain hardening rate at low temperatures is basically resulting effect of two opposite processes: suppression of cross-slip and yield strength increase [25]. In this work, it seems that the latter is attributed to the presence of mobile dislocations in bainite. It is established before that strain hardening rate of the steel increases with increasing pearlite fraction in steel [26]. With considerable pearlite fraction in the structure of steel A19, as opposed to the steel B22, the high strain rate hardening at 77 K is understandable.

According to the classical view on the precipitation hardening, V(C,N) particles precipitated in ferrite coherent or partially coherent with the matrix, possess the highest effect [27], particularly on yield strength [25]. Therefore, it is expected that VN precipitates affect predominantly the strength of steel A19, since it incurporates considerable fraction of ferrite, including both grain boundary ferrite and pearlitic ferrite. On the other hand, in steel B22 where volume fraction of proeutectoid ferrite is lower and the amount of pearlite is almost negligible, hardening contribution of the VN particles should be neglected. The high strain hardening rate of steel A19 and low yield strength compared to B22 seem to disprove this point of view, especially taking into account the notable increase in difference of yield strengths between the two steels at room and at liquid nitrogen temperature (from less than 50 MPa to 120 MPa, Table 3).

There is also an opinion based on thermodynamic calculations that V(C,N) precipitation in austenite region at high temperatures, as in bainite or acicular ferrite at low temperatures is sluggish and that only interphase precipitation during transformation of austenite to ferrite produce particle dispersion capable for significant strengthening effect [16]. More recent findings imply that V(C,N) particles are incoherent even in ferrite [28,29] and that their strengthening contribution is primarily through Orowan-Ashby mechanism of dislocations bypassing the particles [30]. A possibility for this mechanism of strain hardening rate increase observed in steel A19 should be taken into consideration. The observed incoherency leads also to the conclusion that V(C,N) particles precipitated in austenite also could contribute to the strengthening of the steel [31, 32]. Given the similar conditions for precipitation in both steels (same reheating temperature, similar cooling rate, approximate T_{VN}) it doesn't seem that VN particles, presumably precipitated in austenite and thus randomly distributed in overall structure, have an observable influence on strengthening.

Despite the higher level of strain hardening rate, and therefore higher value of strain hardening exponent, *n*, total elongation for steel A19 is low compared to steel B22. Failure of the tensile specimen at the 77K is far beyond tensile instability condition, which is a consequence of the incapacity of the material for further hardening. It is well known that pearlite has a detrimental effect on ductility of the steel, as it brings increased strain hardening rate in combination with numerous potential sites for crack nucleation at ferrite/cementite interfaces [11]. Steep increase of stress in these conditions can give rise to processes of microcracks nucleation whether on cementite lamelaes or at second phase particles. When stress reaches a critical value for fracture, cleavage ensues.

Noticeable differences in yield strength increase when deformation temperature changes from room to liquid nitrogen temperature (47% increase for A19 and 62% for B22, Table 3), cannot be associated only with increased Peierls-Nabarro stress, stress needed for dislocation movement or solid solution strengthening con-

tribution. It is believed that grain refinement and dislocation density are the most effective in strengthening of acicular ferrite or bainitic steels [8,30]. Based on this view and with earlier considerations in mind, it can be assumed that the fine-grained structure of AF alongside with increased dislocation density has more pronounced effect at liquid nitrogen temperature.

The beneficial effect of acicular ferrite on ductility is well documented. Beside benefit of grain refinement at low temperatures, ferrite laths of random spatial orientation force cleavage crack to deflect, spending a considerable part of the energy input [1,2,33]. In classical quenched and tempered medium carbon steels with ferrite-pearlite structure, preferential cleavage nucleation sites are cementinte lamelaes or coarse TiN particles [9]. Giving that steel A19 has a negligible amount of titanium, coarse TiN particles are not expected. Volume fraction of the MnS particles should not be any different in the two steels investigated, as it is already concluded in the case of V(C,N) particles. This leads to conclusion that the main reason for the observed difference in total elongation is probably the presence of pearlite in the structure of steel A19, as opposed to the structure of B22 with acicular ferrite as the predominant constituent.

CONCLUSION

The dominant morphology of the two steels examined after continuous cooling in still air from the austenitization temperature of 1250 °C is acicular ferrite. A considerable fraction of pealite in the microstructure of the V-microalloyed steel A19, as opposed to the almost pearlite free microstructure of the steel Ti-V-microalloyed steel B22, is attributed to the different content of carbon.

The notable differences in deformation behavior of the steels investigated cannot be related just to the different content of carbon and titanium. The high strain hardening rate of steel A19 is attributed to the presence of pearlite in the structure and is concerned to be the main reason for lower tensile ductility. The marked increase of yield strength of steel B22 alongside with higher total elongation than of steel A19 at liquid nitrogen temperature indicates the influence of smaller grain size and high dislocation density of acicular ferrite.

Acknowledgement

The authors are indebted to Ministry of Education, Science and Technological Development of the Republic of Serbia for financial support (Project OI174004) and Serbian Oil Company for supplying experimental material. Abdunnaser Fadel acknowledges the Ministry of Education of Libya for providing PhD scholarship.

REFERENCES

[1] M.A. Linaza, J.L. Romero, J.M. Rodriguez-Ibabe, J.J. Urcola, Improvement of Fracture Toughness of Forging Steels Microalloyed with Titanium by Accelerated Cooling After Hot Working, Scripta Metall. Mater. **29** (1993) 1217–1222.

[2] M.A. Linaza, J.L. Romero, J.M. Rodriguez-Ibabe, J.J. Urcola, Cleavage Fracture of Microalloyed Forging Steels Scripta Metall. Mater. **32** (1995) 395–400.

[3] F. Ishikawa, T. Takahashi, The Formation of Intragranular Ferrite Plates in Medium-carbon Steels for Hot-forging and Its Effect on the Toughness, ISIJ Int. **35** (1995) 1128–1133.

[4] DJ. Drobnjak, A. Koprivica in: C.J. Van Tyne, G. Krauss, D.K. Matlock (Eds.), Microalloyed Bar and Forging Steels, TMS, Golden, 1996, pp. 93–107.

[5] M.J. Balart, C.L. Davis, M. Strangwood, Cleavage initiation in Ti–V–N and V–N microalloyed ferritic – pearlitic forging steels, Mater. Sci. Eng., A **284** (2000) 1–13.

[6] W. Roberts, in: J.M. Gray (Ed.), HSLA Steels Technology and Applications, ASM International, Beijing, 1986, pp. 33.

[7] T. Gladman, in: G. Tither and Z. Shouhua (Eds.), HSLA Steels, Processing, Properties and Applications, TMS, Warrendale, 1992, pp. 3.

[8] H.K.D.H. Bhadeshia, Bainite in Steels: Transformations, Microstructure and Properties, 2nd ed., IOM Communications Ltd., London, 2001.

[9] M.J. Balart, C.L. Davis, M. Strangwood, J.F. Knott, Cleavage Initiation in Ti–V–N and V–N Microalloyed Forging Steels, Mater. Sci. Forum **500**–**501** (2005) 729––736.

[10] A. Koprivica, Structure and properties of medium carbon V-microalloyed steels, PhD Thesis, TMF, Belgrade, 1998 (in Serbian).

[11] H.K.D.H. Bhadeshia, R.W.K. Honeycombe, Steels: Microstructure and Properties, 3rd ed., Elsevier, 2006.

[12] D. Glišić, N. Radović, A. Koprivica, A. Fadel, DJ. Drobnjak, Influence of Reheating Temperature and Vanadium Content on Transformation Behavior and Mechanical Properties of Medium Carbon Forging Steels, ISIJ Int. **50** (2010) 601–606.

[13] A. Fadel, D. Glišić, N. Radović, DJ. Drobnjak, Influence of Cr, Mn and Mo Addition on Structure and Properties of V Microalloyed Medium Carbon Steels, J. Mater. Sci. Technol. **28** (2012) 1053–1058.

[14] C. Capdevila, F. G. Caballero, C. Garcia de Andres, Relevant Aspects of Allotriomorphic and Idiomorphic Ferrite Transformation Kinetics, Mater. Sci. Tech. **19** (2003) 195–201.

[15] C. Capdevila, F.G. Caballero, C. Garcia-Mateo, C. Garciaa de Andres, The Role of Inclusions and Austenite Grain Size on Intragranular Nucleation of Ferrite in Medium Carbon Microalloyed Steels, Mater. Trans. **45** (2004) 2678–2685.

[16] S. Zajac, T. Siwecki, W.B. Hutchinson, R. Lagneborg, Strengthening Mechanisms in Vanadium Microalloyed

Steels Intended for Long Products, ISIJ Int. **38** (1998) 1130–1139.

[17] H. Adrian, in: Microalloying '95, ISS, Warrendale, 1995, pp. 285.

[18] C. Garcia-Mateo, C. Capdevila, F.G. Caballero, C.G.D. Andrés, Influence of V Precipitates on Acicular Ferrite Transformation Part 1: The Role of Nitrogen, ISIJ Int. **48** (2008) 1270–1275.

[19] C. Garcia-Mateo, J. Cornide, C. Capdevila, F.G. Caballero, C.G.D. Andrés, Influence of V Precipitates on Acicular Ferrite Transformation Part 2: Transformation Kinetics, ISIJ Int. **48** (2008) 1276–1279.

[20] H. Adrian, A mechanism for effect of vanadium on hardenability of medium carbon manganese steel, Mater. Sci. Tech. **15** (1999) 366–378.

[21] G. Thewlis, Transformation kinetics of ferrous weld metals, Mater. Sci. Tech. **10** (1994) 110–125.

[22] D.K. Matlock, G. Krauss, J.G. Speer, Microstructures and properties of direct-cooled microalloy forging steels, J. Mater. Process. Tech. **117** (2001) 324–328.

[23] U.F. Kocks, Laws for Work-Hardening and Low-Temperature Creep, J. Eng. Mater. T. ASME **98** (1976) 76–85.

[24] H. Mecking, U.F. Kocks, Kinetics of flow and strain-hardening, Acta Metall. Mater. **29** (1981) 1865–1875.

[25] DJ. Drobnjak, Fizička metalurgija fizika čvrstoće i plastičnosti 1, treće izdanje, TMF, Beograd, 1990 (in Serbian).

[26] K.W. Burns, F.B. Pickering, Deformation and Fracture of Ferrite-Pearlite Structures, J. Iron Steel I. **202** (1964) 899–906.

[27] L. Meyer, C. Strassburger, C. Schneider, in: HSLA Steels: Metallurgy and Applications, J. M. Gray, T. Ko, Z. Shouhua, W. Baorong and X. Xishan (Eds.), American Society for Metals, Metals Park, OH, 1986, pp. 29–44.

[28] E.V. Morales, J. Gallego, H.-J. Kestenbach, On coherent carbonitride precipitation in commercial microalloyed steels, Phil. Mag. Lett. **83** (2003) 79–87.

[29] H.-J. Kestenbach, S.S. Campos, E.V. Morales, Role of interphase precipitation in microalloyed hot strip steels, Mater. Sci. Tech. **22** (2006) 615–626.

[30] A.J. DeArdo, M.J. Hua, K.G. Cho, C.I. Garcia, On strength of microalloyed steels: an interpretive review, Mater. Sci. Tech. **25** (2009) 1074–1082.

[31] H.-J. Kestenbach, J. Gallego, On dispersion hardening of microalloyed hot strip steels by carbonitride precipitation in austenite, Scripta. Mater. **44** (2001) 791–796.

[32] M.D.C. Sobral, P.R. Mei, H.-J. Kestenbach, Mater. Sci. Eng., A **367** (2004), 317–321.

[33] Madariaga I., Gutierez, I., Acicular Ferrite Microstructures and Mechanical Properties in a Medium Carbon Forging Steel, Mater. Sci. Forum **284–286** (1998) 419––426.

ИЗВОД

ДЕФОРМАЦИОНО ПОНАШАЊЕ ДВА КОНТИНУИРАНО ХЛАЂЕНА ВАНАДИЈУМ МИКРОЛЕГИРАНА ЧЕЛИКА НА ТЕМПЕРАТУРИ ТЕЧНОГ АЗОТА

Драгомир М. Глишић, Abdunnaser H. Fadel, Ненад А. Радовић, Ђорђе В. Дробњак, Милорад М. Зрилић

Универзитет у Београду, Технолошко–металуршки факултет, Београд

(Научни рад)

Челици микролегирани ванадијумом и титаном развијани су са циљем да замене каљене и отпуштене средњеугљеничне челике. Иако ове челике карактерише добра комбинација чврстоће и жилавости, с друге стране захтевају накнадну термичку обраду, која значајно повећава трошкове производње. Технологија добијања континуирано хлађених челика треба да обезбеди микроструктуру захтеваних особина после хлађења на ваздуху. Из тог разлога је овим челицима промењен састав, а добре особине се обезбеђују присуством ацикуларног ферита. Ацикуларни ферит карактерише нуклеација унутар претходног аустенитног зрна и велика разлика у кристалографској оријентацији појединих зрна, односно феритних плочица. Ова испреплетана структура обезбеђује повећан отпор кретању прскотине и жилавост која је на нивоу жилавости код традиционалних каљених и отпуштаних челика. У раду су испитивана два континуирано хлађена микролегирана челика са додатком ванадијума. Структура челика без титана и са мањим садржајем угљеника (“A19”) састоји се од континуиране мреже проеутектоидног ферита уз који се издвојио перлит, за којим следи ацикуларни ферит издвојен унутар некадашњег аустенитног зрна. Структура челика са титаном и већим садржајем угљеника (“B22“) састоји се готово у потпуности од ацикуларног ферита. Деформационо понашање на 77 K испитивано је једноосним затезањем. Укупно издужење узорака челика B22 знатно је веће него код челика A19 (10 у односу на 5%). Челик B22 такође поседује већу границу течења и затезну чврстоћу, што је разумљиво с обзиром на већи садржај угљеника. Значајна разлика у дуктилности на температури течног азота у вези је са присуством перлита код челика A19, у односу на структуру ацикуларног ферита код челика B22. Брзина деформационог ојачавања се повећава са повећањем удела перлита у структури, чиме деформација постаје отежана, док истовремено конкурентни процес настајања микропрскотина на кртим цементитним ламелама или честицама секундарних фаза, брзо доводи до кртог лома на 77 K. С друге стране, ацикуларни ферит карактерише повећана густина дислокација, што се манифестује смањењем брзине деформационог ојачавања, а тиме и повећаним капацитетом деформационог ојачавања и већим издужењем код челика B22.

Кључне речи: Средње угљенични челици • Ванадијум микролегирани челици • Ацикуларни ферит • Температура течног азота • Брзина деформационог ојачавања